Spatial distribution of galaxies in the Puppis region

Pierre Chamaraux, Jean-Louis Masnou

Mon. Not. R. Astron. Soc. **347,** 541–555 (2004)

Spatial distribution of galaxies in the Puppis region

Pierre Chamaraux[1]★ and Jean-Louis Masnou[2,3]

[1]*GEPI, Observatoire de Paris, Section de Meudon, 92195 Meudon Cedex, France*
[2]*Observatoire de Bordeaux, Université Bordeaux 1, B.P. 89 33270 Floirac, France*
[3]*LUTH, Observatoire de Paris, Section de Meudon, 92195 Meudon Cedex, France*

Accepted 2003 September 17. Received 2003 September 16; in original form 2001 July 6

ABSTRACT

We determine the spatial distribution of the galaxies located behind the part of the zone of avoidance of the Milky Way defined by $220^\circ < l < 260^\circ$, $|b| < 20^\circ$, $\delta \leqslant 0^\circ$, up to a distance of 8000 km s^{-1}. We use a sample of 369 galaxies with measured redshifts, of which 97 have been detected with the Nançay radio telescope. We show that our sample can be considered to be complete in apparent diameter down to 1.9 arcmin, a property that allows us to correct the density of galaxies for the loss of objects with distance. We then search for groups of galaxies using a companionship method and find 12 groups with at least five members, of which five are new. The members of one group are H I deficient by a factor of 1.6 on average. The method is then used to search for large structures and allows us to characterize the Puppis wall at $1400 < V_0 < 2600$ km s^{-1}; it is 30 Mpc long, with the main axis being parallel to the sky plane, and it connects the Antlia cluster to the Fornax cluster through the zone of avoidance. The density of galaxies in the wall is approximately 20 times the general density of galaxies, i.e. half that observed in the densest part of the Pisces–Perseus supercluster. No internal motions are found along the line of sight, indicating that the Puppis wall has not yet collapsed.

Key words: galaxies: clusters: general – galaxies: clusters: individual: Puppis.

1 INTRODUCTION

The Milky Way strongly absorbs the light of the galaxies located at low galactic latitudes, i.e. at $|b| < 15^\circ$, preventing us from obtaining complete knowledge of their distribution, despite the considerable progress achieved during the last decade. However, knowledge of the whole sky distribution of relatively nearby galaxies is necessary for solving important questions, among which are: (i) the accurate determination of a few nearby large-scale structures, which seem to go across the galactic plane, such as the Local Supercluster and the Pisces–Perseus chain; (ii) the origin of the peculiar velocity of the Local Group, found from the dipole anisotropy of the cosmic microwave background, and for which the presence of unknown nearby objects could play an essential part; (iii) the streaming motion due to the Great Attractor, the centre of which is hypothesized to be located behind the Milky Way (Kolatt, Dekel & Lahav 1995).

Much progress has been recently achieved towards the solution of these problems, thanks to considerable unveiling of the zone of obscuration (ZOA), in particular at optical wavelengths, for which the area of the ZOA has decreased by more than a factor of 2 (see the review paper by Kraan-Korteweg & Lahav 2000).

★E-mail: Pierre.Chamaraux@obspm.fr

During the last few years, we have focused on the Puppis zone: $230^\circ < l < 260^\circ$, $|b| < 15^\circ$, where the galactic absorption is relatively small ($A_B < 3$ mag). In Yamada et al. (1994), we have used 129 *IRAS* galaxies with $f_{60\,\mu m} > 0.6$ Jy to study the spatial distribution of the galaxies in that region, obtaining a good determination of the Puppis cluster, at 2000 km s^{-1}; this cluster had already been brought to light by Lahav et al. (1993) who had shown that it is second in importance, after the Virgo one, up to 3000 km s^{-1}, and that it could bring a significant contribution to the motion of the Local Group perpendicular to the Supergalactic Plane.

On the other hand, we have measured 101 galaxies in that region using the H I 21-cm line, of which 47 had no known recession velocity (Chamaraux et al. 1999, hereafter Paper I). In the present paper, those measurements and all the existing other ones are gathered to study the spatial distribution of the galaxies in the zone: $220^\circ < l < 260^\circ$, $|b| < 20^\circ$, $\delta \leqslant 0^\circ$, up to 8000 km s^{-1}; this provides a sample of 369 objects, the distances of which are computed by the Hubble law.

The paper is organized as follows. In Section 2, the sample is defined and is shown to be roughly equivalent to a sample complete for apparent diameters down to 1.9 arcmin. In Section 3, we sort out the groups of galaxies with a companionship method. Large-scale distribution is examined in Section 4, leading to accurate determination of the Puppis wall; quantitative study shows that its density is half that found in the densest part of

the Pisces–Perseus supercluster. Section 5 gives a summary and a conclusion.

2 THE SAMPLE OF GALAXIES

2.1 Definition of the sample

Our purpose is to study the spatial distribution of galaxies, mainly in the zone (hereafter zone A): $220^\circ < l < 260^\circ$, $|b| < 20^\circ$, $\delta \leqslant 0^\circ$. We compute the distances of the objects by the Hubble law from the recession velocities V_0 referred to the centroid of the Local Group (Paper I); a Hubble constant $H_0 = 75$ km s^{-1} Mpc^{-1} is used in agreement with the recent determination by Jensen et al. (2001). We limit our study to galaxies with $V_0 < 8000$ km s^{-1}, which comprise the majority of the available objects, in particular all 97 galaxies included in Paper I. In order to trace possible large-scale structures, we extended the zone studied to the larger region (hereafter zone B): $205^\circ < l < 260^\circ$, $|b| < 35^\circ$, $\delta \leqslant 0^\circ$. Thus, our sample of galaxies is comprised of all available objects in that region having a known recession velocity $V_0 < 8000$ km s^{-1}, namely 624 galaxies, 369 of which are in zone A.

The recession velocities are extracted from seven sources listed in Table 1.

This table also provides the range covered in l and b within zone B by each source (columns 2 and 3), the selection criteria (column 4), the type of redshift measurement, i.e. H I 21-cm or optical lines (column 5), and finally the number of sample galaxies taken from each source in zone B (column 6) and in zone A (column 7). Of course, many galaxies of our sample are listed in more than one source; in such a case, the redshift has been taken from the first of the sources appearing in Table 1, by order of increasing source number. H I redshifts have been systematically preferred if available, since they are more accurate than optical ones. This method leads to the numbers given in columns (6) and (7). Note that in zone A, our zone of main interest, the richest source of redshifts is Paper I (25 per cent of our total sample), which justifies that the present study follows up Paper I. A plot of the 624 galaxies of our sample is shown in Fig. 1, in galactic coordinates.

2.2 Diameter completeness of the sample

The purpose of the present work consists in determining the spatial distribution of galaxies in zone A, mainly in order to display structures such as clusters and voids. Such a study requires the computation of the density in galaxies at any point M of the zone. Of course any sample of galaxies cannot include all the objects around M, because of the observational limitations. However, it is sufficient for the computation of the density that the sample contains a known fraction of the galaxies and not all of them (this fraction can depend on the distance to the point M). That requirement is satisfied in particular for a sample that is complete in apparent magnitudes or in apparent diameters, an usual situation in that kind of studies, which we examine below in the case of the present sample.

More explicitly, consider for instance a sample of galaxies that is complete in apparent diameters a down to the limit a_0. One can then compute the number density $\rho_{a \geqslant a_0}(M)$ in galaxies having $a \geqslant a_0$ close to each point M. Using the cumulative galaxy linear diameter function $\Phi(\geqslant A)$, one can then determine the density in galaxies $\rho(M)$ through

$$\rho(M) = \rho_{a \geqslant a_0}(M) \frac{\Phi(\geqslant A_m)}{\Phi(\geqslant A_0(\Delta))}, \tag{1}$$

where A_m is the linear diameter of the smallest galaxy used in the determination of the diameter function; $A_0(\Delta)$ is the linear diameter of a galaxy seen at the distance Δ of M with an apparent diameter a_0.

Therefore, the density in galaxies $\rho(M)$ can be entirely computed from the data for a sample complete in apparent diameters. Note, however, that if Δ is quite large, the ratio $\Phi(\geqslant A_m)/\Phi(\geqslant A_0(\Delta))$ has a high value, resulting in a large uncertainty on $\rho(M)$. However, what is important in the study of the distribution of galaxies is to obtain accurate ratios of the densities at the different points of the region. This requirement is satisfied if the values of $\Phi(\geqslant A_0(\Delta))$, and therefore the distances Δ do not vary too much within the region investigated.

Thus it is clear that it is worthwhile to carry out a study of the completeness of our sample for an evaluation of the correctness of the determination of the spatial distribution of the galaxies in the zone concerned.

We choose to study the completeness in apparent diameters; indeed most of our sample galaxies are listed in the ESO catalogue, which provides the apparent diameter for each entry. Moreover, 80 per cent of the sample galaxies are 60-μm flux-limited or apparent diameter-limited (see Table 1); since there is some correlation between the 60-μm flux and the apparent diameter, one can expect some completeness in apparent diameters for our sample.

We have performed the completeness study in zone A, after removal of the strip $-7^\circ < b < +4^\circ$. Indeed, for very low values of $|b|$, the galactic extinction leads to large reductions of the galaxy diameters, which can reach a factor of 10; thus, even sample galaxies having large unabsorbed apparent diameters can disappear from the ESO catalogue, the diameter limit of which is one arcmin, and then the completeness cannot be studied correctly from this catalogue at these low galactic latitudes.

In the defined region, we have gathered all the ESO galaxies having an apparent diameter corrected for galactic absorption

Table 1. Sources of redshifts for the galaxies of our sample.

Source (1)	l range (2)	b range (3)	Selection (4)	Measurement (5)	N_B (6)	N_A (7)
(1)	(235°, 260°)	$\|b\| < 13^\circ$	$\Phi_{ESO} \geqslant 1.6$ arcmin	H I	101	97
(2)	(235°, 255°)	$\|b\| < 8^\circ$	–	H I	13	13
(3)	(230°, 260°)	$\|b\| < 15^\circ$	$f_{60\mu m} > 0.6$ Jy	Optical	72	72
(4)	(220°, 260°)	$15^\circ \leqslant \|b\| < 25^\circ$	$f_{60\mu m} > 0.5$ Jy	Optical	96	67
(5)	All	All	–	Optical, H I	272	77
(6)	All	$\|b\| < 15^\circ$	$f_{60\mu m} > 0.6$ Jy	Optical	48	38
(7)	All	$\|b\| > 5^\circ$	$f_{60\mu m} > 1.2$ Jy	Optical	22	5

Source (1) Paper I; (2) Kraan-Korteweg & Huchtmeier (1992); (3) Yamada et al. (1994); (4) R. S. Saunders (1996, private communication); (5) Fairall (1995); (6) Visvanathan & Yamada (1996); (7) Fisher et al. (1995).

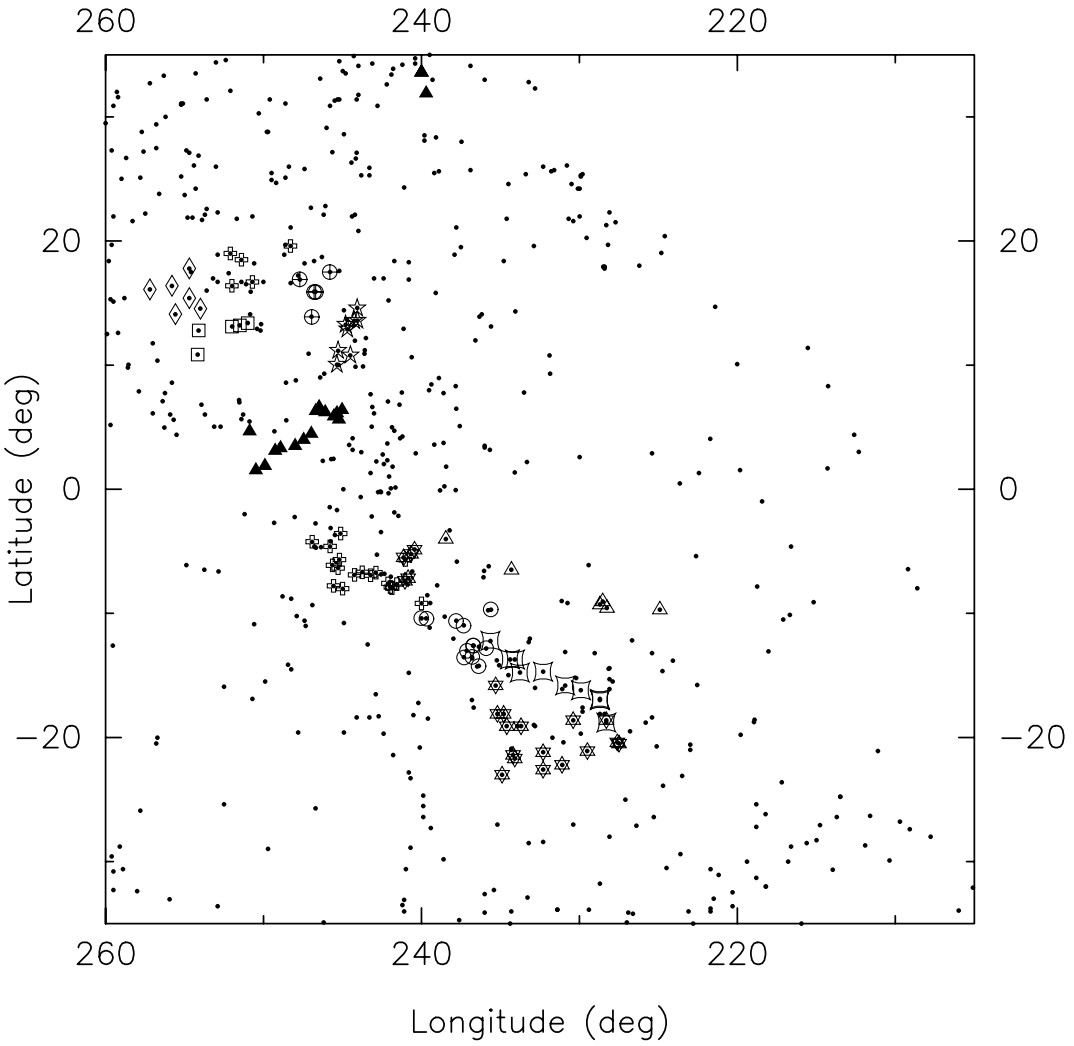

Figure 1. Plot of the 624 galaxies of our sample in galactic coordinates. The zone covered by the sample is defined by $205^\circ < l < 260^\circ$, $|b| < 35^\circ$ and $\delta < 0^\circ$. Galaxies pertaining to a group of at least five members are designated by a specific symbol other than a simple dot.

$a_c \geqslant 1.6$ arcmin (our sample is severely incomplete below this value of the diameter). The corrections for galactic absorption on the diameters range from 2 to 8 per cent; these are quite small corrections, resulting from a galactic absorption lower than 0.6 mag (see Paper I for the computation of the correction). Consequently, all the galaxies of the region having $a_c \geqslant 1.1$ arcmin are listed in the ESO catalogue, which is complete down to an uncorrected diameter limit of 1.0 arcmin; this is also a fortiori the case for the galaxies having $a_c \geqslant 1.6$ arcmin. So the completeness factor of our sample for a corrected diameter $a_c \geqslant 1.6$ arcmin in the region considered is simply given by the percentage of ESO galaxies having this diameter and included in our sample. Since the diameter corrections are small, it is unnecessary to compute the value of a_c for each galaxy to obtain the completeness, which would be a long and tedious work. Instead, we have determined the percentage of ESO galaxies in our sample at each value of the uncorrected diameter, from which we have derived statistically the completeness factor at each value of a_c.

As a result, we find that our sample is 60 per cent complete for $a_c \geqslant 1.9$ arcmin in the whole region concerned; this completeness suddenly decreases to less than 30 per cent for $a_c \leqslant 1.8$ arcmin. Quite remarkably, the completeness is the same for each apparent diameter in the range (1.9, 5.0 arcmin). For $a_c \geqslant 5.4$ arcmin, our sample is complete, but only 9 per cent of the galaxies with $a_c \geqslant 1.9$ arcmin have such large diameters.

Also note that completeness is expected to be quite uniform within the whole region studied. Indeed, the majority of the sample galaxies have been picked uniformly by the optical identification of 60-μm flux-limited *IRAS* point sources; hence the uniform apparent diameter completeness through the correlation between $f_{60\mu m}$ and a.

For $|b| \geqslant 25^\circ$, there are only two sources of redshift available (see Table 1), and there is not any interesting completeness property.

What about the completeness in the zone $220^\circ < l < 260^\circ$, $-7^\circ < b < +4^\circ$? For $220^\circ < l < 235^\circ$ and $250^\circ < l < 260^\circ$, almost all the sample objects have been selected by *IRAS* criteria; for $235^\circ < l < 250^\circ$, 40 per cent of them have been selected this way; the other 60 per cent have been mainly selected from their apparent diameter (source 1). In the work of galaxy identification of *IRAS* sources carried out by Yamada et al. (1993) and of subsequent redshift measurements by Visvanathan & Yamada (1996), there appears to be a clear lack in identified galaxies for $|b| < 5^\circ$ and $220^\circ < l < 260^\circ$, except at $235^\circ < l < 250^\circ$ (see fig. 1 in Visvanathan & Yamada 1996); this gap is also obvious in our Fig. 1. As a matter of fact, galactic extinction in that zone can exceed four magnitudes,

leading to a decrease of apparent diameters by a factor larger than 10, as above-mentioned, which prevents secure identification of most galaxies. However, for $235^\circ < l < 250^\circ$, the galactic extinction is always lower than three magnitudes, and the corresponding decrease of apparent diameters never exceeds a factor of 4; thus a galaxy having an unabsorbed apparent diameter larger than the completeness limit 1.9 arcmin found in the remainder of zone A will have an absorbed diameter of 0.5 arcmin at least. That allows for easy identification. Thus one can expect the same completeness to $a_c = 1.9$ arcmin for *IRAS* sources in that region as in the remainder of zone A. It also seems to be the case for the objects of source (1), since the plot $\log N(\geqslant a_c)$ is linear in that region to $a_c = 1.9$ arcmin.

Thus our sample is 60 per cent complete to $a_c = 1.9$ arcmin in the whole zone A, except in the two regions of very low galactic latitudes $-7^\circ < b < +4^\circ$ at $220^\circ < l < 235^\circ$ and $250^\circ < l < 260^\circ$, respectively, which represent less than 20 per cent of the zone. Outside zone A, i.e. in the remainder of zone B, the sample has no significant completeness characteristics.

The fact that our sample exhibits the same value of completeness for any diameter a larger than $a_0 = 1.9$ arcmin has an important consequence. Hereafter the apparent diameters a refer to diameters corrected for galactic extinction, which have been noted a_c above; the index c has been omitted for simplification and since there is no ambiguity. Namely one can compute the galaxy density $\rho(M)$ from the density $\rho^s_{a\geqslant a_0}(M)$ in galaxies of our sample having $a \geqslant a_0$.

Indeed, let $\rho_{a\geqslant a_0}(M)$ be the total density at M in galaxies having a diameter larger than a_0 (i.e. corresponding to a complete sample). One can write

$$\rho_{a\geqslant a_0}(M) = \sum_{a_i \geqslant a_0} \underline{\rho}_{a_i}(M),$$

where $\underline{\rho}_{a_i}$ is the density in galaxies of diameter a_i of the complete sample.

The same equation holds between $\rho^s_{a\geqslant a_0}(M)$ and $\underline{\rho}^s_{a_i}(M)$, where $\underline{\rho}^s_{a_i}(M)$ is the density of our sample galaxies having a diameter a_i. The constant value of the completeness factor of our sample for any a_i greater than a_0 through the whole zone A leads to: $\underline{\rho}^s_{a_i}(M) = 0.6\underline{\rho}_{a_i}(M)$. Hence, $\rho^s_{a\geqslant a_0}(M) = 0.6\rho_{a\geqslant a_0}(M)$.

Therefore, the density in zone A of our sample galaxies having $a \geqslant 1.9$ arcmin is the same as that obtained from a sample which is complete to a_0, except for the presence of a uniform multiplicative factor of 0.6, hence $\rho(M)$ from equation (1).

However, there is still an interesting useful property of our whole sample. Indeed, let us examine the proportion of 'large' galaxies of our sample, i.e. those galaxies having a larger than the limit 1.9 arcmin of partial completeness. Such a proportion is of course expected to depend on the redshift, since the fraction of large galaxies decreases with distance. In turn, it is expected to be independent of the position within zone A at a fixed distance, since most of our sample galaxies have been selected according to criteria (fluxes $f_{60\mu m}$, apparent diameters), which have been applied uniformly in the whole region.

Thus we have determined the proportion of large galaxies separately by redshift slices of 1000 km s^{-1}. We find that it has a constant value of 60 per cent in each redshift slice for $V_0 < 3000$ km s^{-1}. Beyond this velocity, the sample is too poor to draw any conclusion. In fact, given the range of the apparent diameters of our sample galaxies (mainly from 1.2 to 2.8 arcmin), their linear diameters are small for $V_0 < 3000$ km s^{-1}. For these values of the linear diameters, the diameter function is almost flat (see fig. A2 in Lahav, Rowan-Robinson & Lynden-Bell 1988); which explains why the proportion of large galaxies is constant in this redshift range.

Thus we can conclude that the galaxy distribution obtained from our sample in zone A to a distance of 3000 km s^{-1} is the same as that which would be found from a sample complete in apparent diameter to $a_0 = 1.9$ arcmin, if we assume that the spatial distributions of large and smaller galaxies are not significantly different up to that distance. Here, there is no longer a constant multiplicative factor between the two distributions.

Indeed, the total number of galaxies present in our sample at each distance is equal to 1.67 times the number of the sample objects having $a \geqslant a_0$; it happens to be exactly the number of galaxies in the complete sample, since our sample completeness factor down to a_0 is 60 per cent.

Therefore, for the study of the galaxy distribution, we can reasonably treat our sample as complete up to $V_0 = 3000$ km s^{-1} in zone A. As it is seen below, all the structures of interest found from our sample are, in fact, within this distance range. On the other hand, the corrections for the loss of objects can be performed confidently up to that distance, since they are not too large.

To end the present section, note that the diameter completeness can be transformed into a magnitude completeness. Indeed, as shown by Lahav et al. (1988), there is a tight correlation between the ESO diameter a and the total magnitude B_T of a galaxy, namely: $B_T = 15.43 - 5\log(a)$, with a in arcmin. Taking into account the average relation $B(0) - B_T = 0.5$ (de Vaucouleurs et al. 1976), one then finds that the corresponding magnitude completeness limit of our sample in zone A is $B(0) = 14.5$.

3 SMALL-SCALE SPATIAL DISTRIBUTION OF GALAXIES IN THE PUPPIS REGION

We now present the spatial distribution of the sample galaxies from their positions and their redshifts. We first look for the small-scale distribution, i.e. we sort out the physical groups of galaxies present in our sample. We then study the large-scale distribution of the sample galaxies, i.e. we investigate the large structures of supercluster type in the region concerned and its surroundings.

3.1 Search for groups of galaxies

Four groups of galaxies have been previously recognized in zone A by visual inspection of galaxy plots; these are Puppis A (245°, −7°) at $cz \sim 2000$ km s^{-1}, Puppis B (237°, −15°) at $cz \sim 2000$ km s^{-1} (Yamada et al. 1994), the group (246°, +5°) at $cz \sim 1400$ km s^{-1} (Kraan-Korteweg & Huchtmeier 1992, hereafter KH; Yamada et al. 1994) and group (246°, +2.5°) at $V_0 \sim 750$ km s^{-1} (KH).

Since our sample of galaxies with known redshifts is much more extensive than in the previous studies, here we can carry out a systematic search for groups by using an objective clustering method.

Before discussing the available clustering methods, it must be emphasized that the results obtained by any of them are only reliable when one uses a complete sample. Indeed, only in that case can one accurately perform the necessary corrections in order to take into account the loss of galaxies with increasing distances, so that groups located at different distances can be compared without introduction of bias; moreover, the population of a group can be defined quantitatively without any inaccuracy. Now, as shown in the previous section, our galaxy sample in zone A indeed has the properties of a complete sample for apparent diameter up to a distance of 3000 km s^{-1}.

Concerning the available clustering techniques, they belong to two classes: the hierarchical one, introduced by Materne (1978), and subsequently developed by Tully (1987) and Gourgoulhon, Chamaraux & Fouqué (1992, hereafter GCF) and the companionship method introduced by Huchra & Geller (1982, hereafter HG). The advantage of the hierarchical method is that it provides not only the groups themselves, but also the more extended aggregates that contain them, the groups often displaying a core–halo structure. Despite this advantage, we have decided to choose HG's method, which is much easier to handle.

In HG's method, a galaxy i of the sample not previously catalogued in a group is examined for companions j defined in such a way that their projected distance D_{ij} to i and their recession velocity difference $|V_i - V_j|$ are, respectively, lower than given values, D_L and V_L, namely

$$D_{ij} = 2\,\sin(\theta_{ij}/2)\frac{(V_i + V_j)}{2H_0} < D_L \tag{2}$$

$$|V_i - V_j| < V_L, \tag{3}$$

where θ_{ij} is the angular separation between i and j. V_i and V_j are referred to the centroid of the Local Group, and H_0 is the Hubble constant.

Companions are then examined for second-order companions, and so on until no more companions are found. The entity formed by the whole set comprising the galaxy i and all its companions of any order then defines a new group of galaxies.

Use of HG's method requires us to choose defined values for the parameters D_L and V_L. Before giving the values adopted in the present study, note that D_L has to be scaled with the distance $\Delta_{ij} = (V_i + V_j)/2H_0$ to the galaxies; indeed a given group put away at a larger distance will contain fewer visible galaxies, so the projected distance from a galaxy to its nearest group companion will be larger on average, and D_L will have to be increased accordingly if one wishes to sort out the same group. In turn, V_L has to be taken independent of Δ_{ij}. Indeed, the average velocity difference between any two physical members of a given group only depends on the velocity dispersion σ_V within the group, and not on the number of members nor on the position nor on the luminosities or diameters of these two galaxies. If a given group is put away at a larger distance, its velocity dispersion measured from the redshifts of the visible galaxies will remain the same, since relative motions of galaxies within the group are independent of their luminosities or diameters; therefore V_L has to be assigned a fixed value if one wishes to obtain the same group, independent of its distance.

For a sample of galaxies complete to a limiting apparent diameter a_0 (in arcmin), one finds for D_L as a function of the distance Δ_{ij} (see GCF)

$$D_L(\Delta_{ij}) = D_L(\Delta_0)\frac{f(\Delta_{ij})}{f(\Delta_0)} \tag{4}$$

with

$$f(\Delta_{ij}) = \left[\int_{D(\Delta_{ij})}^{+\infty} \Phi(D)\,\mathrm{d}D\right]^{-1/2} = [\Phi(\geqslant D(\Delta_{ij}))]^{-1/2},$$

where $D(\Delta_{ij})$ is the minimum linear diameter of a sample galaxy at the distance Δ_{ij}, i.e. $D(\Delta_{ij}) = a_0(V_i + V_j)/2$ in km s$^{-1}\times$ arcmin. Δ_0 is a reference distance, for instance that corresponding to $V_0 =$ 1000 km s^{-1}. $\Phi(D)$ is the galaxy linear diameter function.

$\Phi(\geqslant D)$ is the cumulative galaxy linear diameter function of galaxies, for which we use the analytical form found by Lahav et al. (1988) for the ESO diameters, namely

$$\Phi(\geqslant D) = \Phi_* t^{-\mu}\left(1 + \frac{t}{\nu}\right)^{-\nu},$$

where $\mu = 0.2$, $\nu = 3.4$ and t is defined by $t = (D/D_*)^2$, with $D_* = 6973$ km s^{-1} arcmin. [Later on, Hudson & Lynden-Bell 1991 derived another simpler analytic formula for $\Phi(\geqslant D)$, which takes into account the incompleteness of the redshift surveys for uncorrected apparent diameters; however, use of this improved expression does not significantly change our results.]

Taking the completeness limit $a_0 = 1.9$ arcmin found above for zone A, we obtain

$$t(\Delta_{ij}) = \left[2.72 \times 10^{-4}\frac{(V_i + V_j)}{2}\right]^2.$$

Hence the scaling of D_L used in the research of the groups in the Puppis zone. Note that $f(\Delta_{ij})/f(\Delta_0)$ varies from 0.85 to 1.44 for distances increasing from 500 to 2500 km s^{-1}, which is the distance range where our groups are found; so the scaling is far from negligible.

Also note that the distance scaling given by HG is incorrect, as also is their V_L scaling with the distance (see GCF for the detailed discussion).

Finally, we have to fix the values of $D_0 = D_L(\Delta_0)$ and of V_L. As a matter of fact, these two quantities are the only free parameters in HG's method. Their choice has an obvious effect on the average characteristics of the groups, since V_L is related to their velocity dispersions and D_0 to their dimensions. Too small values of D_0 lead to splitting of physical groups into several parts, whereas too large ones lead to merging together of unrelated groups. Of course D_0 also depends on the limiting apparent diameter for a sample complete in apparent diameter, contrary to V_L.

For D_0, we have tried several values between 0.5 and 0.9 Mpc. The most satisfactory choice for our sample was $D_0 = 0.84$ Mpc, which was adopted, and which is the same value as that taken by HG for our H_0 value.

Our choice of V_L was guided by the requirement to obtain groups similar to those in GCF, for which the one-dimensional (1D) velocity dispersions are $\sigma_V < 150$ km s^{-1}, due to the density limit used to define the groups in that study. We have tried $V_L = 75$, 150, 300 and 600 km s^{-1}, and, as expected, values of $\sigma_V < 150$ km s^{-1} were obtained for $V_L = 150$ km s^{-1}, a limit velocity that was then adopted. Note that HG use $V_L(\Delta_0) = 400$ km s^{-1} (V_L is function of the distance in HG), resulting in much larger velocity dispersions within their groups.

3.2 The groups of galaxies in the Puppis region

The modified HG's method was applied to our basic sample of 624 galaxies having $V_0 < 8000$ km s^{-1}, in order to sort out the groups of galaxies in the whole zone B. However, as emphasized in the previous section, the groups found that way are fully reliable in zone A only, for $V_0 < 3000$ km s^{-1}, where our galaxy sample has the characteristics of a complete one.

With these words of caution in mind, we now present our results. 42 groups containing at least three galaxies were identified in zone B. Table 2 displays the number of groups having a population higher than a given value and the pairs of galaxies as well; note that the most populated group contains 18 members.

Fig. 1 displays the 13 groups located in zone B and containing at least five members; the different groups are marked by different

Table 2. Number of groups in zone B containing at least N galaxies (comprising pairs of galaxies).

Number of galaxies N	2	3	4	5	6	7	8	9	10
Number of groups	107	42	23	13	8	6	6	5	5
Number of galaxies N	11	12	13	14	15	16	17	18	
Number of groups	4	4	3	3	3	3	1	1	

Table 3. Physical parameters of the groups in zone A.

Group (1)	l (2)	b (3)	N (4)	$\bar{V}_0$ (5)	σ_V (6)	R_V (7)	t_{cr} (8)	M (9)	$N_{7.4}$ (10)
1	232.2	−20.1	16	1485	132	1.3	5.8	35	20
2	231.7	−15.4	10	2525	53	1.5	24.0	7	21
3	237.3	−12.0	12	1891	128	0.6	4.6	15	19
4	230.5	−8.0	6	536	41	0.3	10.0	0.95	4
5	243.7	−6.6	18	1786	202	1.2	3.4	70	27
6	240.8	−6.0	5	7138	96	2.2	13	35	–
7	247.4	+4.7	16	1385	103	0.7	5.5	11	19
8	244.6	+12.5	8	1461	79	0.6	4.7	6	10
9	252.6	+12.7	5	1705	47	0.8	9.4	3	7
10	255.3	+15.7	6	2047	96	1.5	5.4	23	10
11	246.8	+16.0	5	2335	110	0.6	4.7	12	10
12	250.9	+18.0	5	517	70	0.4	2.2	3	4

Column (1) rank of the group by order of increasing galactic latitude. (2) Galactic longitude l of the group centre (deg). (3) Galactic latitude b of the group centre (deg). (4) Number N of members of the group pertaining to our sample. (5) $\bar{V}_0$, recession velocity of the group centre (km s^{-1}), referred to the centroid of the Local Group [$V_0 = V_h + 300 \sin(l) \cos(b)$, where V_h is the heliocentric recession velocity]. (6) σ_V, 1D velocity dispersion of the group (km s^{-1}). (7) R_V, virial radius (Mpc). (8) t_{cr}, crossing time in units of 10^9 yr. (9) Mass of the group in units of 10^{12} solar masses. (10) Estimated number of members of the group, referred to the same limiting linear diameter $A_0 = 7.4$ kpc.

symbols. The filled dots represent sample galaxies not included in any of those groups. Note that most of the groups are located in a narrow band.

For each group, we have computed the physical parameters of interest, namely the virial mass, the radius, the velocity dispersion and the crossing time, each of those quantities being defined as in GCF. Since we are primarily interested in the groups located in the zone of avoidance (the other ones are generally known), and since our sample is not complete outside zone A, we give these parameters in Table 3 uniquely for the 12 groups located in zone A and containing at least five members. For those groups, which are ordered by increasing galactic latitude in Table 3, we also provide the populations, the positions and the recession velocities; the list of their members is given in Table 4.

One can see that all the groups but one (number 6) have $V_0 <$ 3000 km s^{-1}, i.e. belong to the region of space where our sample is equivalent to a complete one. Thus it makes sense to compare the populations of the different groups in galaxies having linear diameters larger than a fixed one A_0. We have chosen $A_0 = 7.4$ kpc, which corresponds to $a_0 = 1.9$ arcmin at $V_0 = 1000$ km s^{-1}. The populations of the groups have then been corrected using Lahav et al.'s (1988) diameter function, leading to the values given in the last column of Table 3. No value is given for group number 6, because of sample incompleteness at its distance and to the inaccuracy of the very large distance correction needed; the value provided for group number 1, which lies partially outside zone A, should be taken with some caution.

Inspection of the positions and recession velocities shows that three of our groups coincide with groups found previously by visual examination, namely groups 5 and 3, corresponding, respectively, to Puppis A and Puppis B in Yamada et al. (1994) and group 7 given by KH. On the other hand, groups 1, 2, 3, 7, 8 and 12 can be found in GCF and Fouqué et al. (1992) with the respective names: N2217, N2207, N2280 (association 17), N2559, E 563–016 and N2835. So here we are sorting out five new groups containing at least five members, namely groups 4, 6, 9, 10 and 11.

Examination of Table 3 shows that seven among the 12 groups have recession velocities in the narrow range [1300, 2100 km s^{-1}]; a result that indicates a significant spatial concentration, which will be discussed below. Also note that all the groups but one have 1D velocity dispersions $\sigma_V \leqslant 150$ km s^{-1}, as those found in GCF; the remaining group is, in fact, quite massive.

It is also significant that all the groups except one have crossing times lower than the age of the Universe and thus probably represent actual physical groups. The only exception is group 2; examination of this group shows it is an almost linear structure comprising 10 galaxies, which present nearly equal redshifts, diameter of which is approximately 5 Mpc; such a dimension is definitely too large for a group; this peculiarity, added to the very low velocity dispersion of this structure, seems to indicate that we are not concerned with a physical group, but rather with a kind of filament of galaxies not gravitationally bound; the absence of any velocity gradient along the structure shows that this filament is perpendicular to the line of sight.

Another interesting point is that groups 5 and 3 are spatially very close, and could thus form a single unit, with two density concentrations. If we merge those two groups, we obtain a group with $\sigma_V \approx 200$ km s^{-1} and a population of 46 galaxies having linear diameters larger than 7.4 kpc, which compares well with the Fornax cluster (55 galaxies with the same characteristics from GCF), except that the latter is more massive, with $\sigma_V \approx 300$ km s^{-1}.

At last, note that group number 6, at $l = 241^\circ$, $b = -6^\circ$ and $V_0 \approx 7100$ km s^{-1} is a subset of a concentration of galaxies at $V_0 \approx 7200$ km s^{-1} discovered by Visvanathan & Yamada (1996).

To end this section, note that the groups found here compare well with GCF groups containing five galaxies at least located at a distance lower than 40 Mpc; the median values of their parameters are: $\sigma_V = 80$ km s^{-1}, $R_V = 0.69$ Mpc and $t_{cr} = 3.3$ Gyr, compared with $\sigma_V = 96$ km s^{-1}, $R_V = 0.8$ Mpc and $t_{cr} = 5.4$ Gyr for the present sample; this result shows that those respective groups are of the same nature, although obtained by two different methods.

3.3 An H I deficient group?

It is now firmly established that spiral galaxies of several clusters have H I contents much lower than those of isolated galaxies (Haynes & Giovanelli 1984). Such an H I deficiency can reach a factor of 4 and affects members of those clusters, which contain intracluster gas, the presence of which is revealed by its X-ray emission; it is interpreted as being due to the removal of interstellar gas from galaxies in their motion through the intracluster medium. Systematic H I deficiencies of a factor of 2 on average have also been found in galaxies members of Hickson compact groups (Williams & Rood 1987), 75 per cent of which contain hot intragroup gas (Ponman et al. 1996). However, as far as we know, no H I deficiency has been noted up to now in any loose group of galaxies, although many of them contain hot intragroup gas too (Mulchaey et al. 1996). This question will be examined again at the end of the present section.

Table 4. List of members of the 12 groups given in Table 3.

Group 1:
E425-002 E425-008 E426-001 E488-049 E488-060 E489-015 E489-022 E489-029
E490-010 E555-019 E555-022 E555-039 I2158 N2131 N2139 N2217
Group 2:
E490-007 E490-014 E490-020 E490-046 I2163 N2179 N2207 N2216 N2223 N2263
Group 3:
A06554-2427 E427-002 E427-026 E490-028 E490-036 E490-041 E490-044 E491-009
N2292 N2293 N2325 P19917
Group 4:
CG1 260 CG1 381 CG2 2870 E558-011 I2171 N2283
Group 5:
CG2 980 CG2 1055 CG2 1113 CG2 1147 E427-034 E428-014 E428-015 E428-016
E428-020 E428-025 E428-028 E428-029 E428-031 E428-032 E428-033 E428-037
E429-001 N2380
Group 6:
E428-016 E428-019 E492-014 IR07229-2725 IR07239-2631
Group 7:
CG2 2865 E430-026 E430-030 E431-001 E431-002 E431-010 E494-040 E495-005
E495-006 E495-009 E495-011 E495-012 I2311 N2559 N2566 P23156
Group 8:
E562-019 E563-002 E563-012 E563-013 E563-014 E563-016 N2613 N2665
Group 9:
E432-015 E433-002 E497-001 E497-002 IR08574-2510
Group 10:
E433-010 E497-022 E498-003 E498-005 N2821 N2888
Group 11:
E563-028 E563-034 E563-036 E564-004 E564-011
Group 12:
E497-017 E564-030 E565-001 N2784 N2835

CG1, catalogue of galaxies behind the Milky Way (Saitō et al. 1990).
CG2, catalogue of galaxies behind the Milky Way (Saitō et al. 1991).
E for ESO, I for IC, IR for IRAS, N for NGC, P for PGC.

In the Puppis region, we have sorted out several groups of galaxies, two of which (groups 3 and 5) seem to represent objects that are intermediate between groups and clusters. H I contents have been measured in many members of those groups (see Paper I). Thus it is worthwhile to carry out a systematic study of these H I contents. For this study, we compute for each galaxy concerned the quantity $def = \log M_{\rm H} - \overline{\log M_{\rm H}}$, where $M_{\rm H}$ is the H I mass of the galaxy and $\overline{\log M_{\rm H}}$ is the logarithm of the H I mass expected for an isolated galaxy having the same linear diameter as the galaxy considered, and taken from Haynes & Giovanelli's (1984) study (see Paper I). A significantly negative value of *def* points towards an H I deficiency in the galaxy considered.

The best candidates a priori for an H I deficiency are the groups 3 and 5, which are the richest among the groups found, and the population of which could be as important as half that of the Virgo cluster (Yamada et al. 1994), this cluster itself being H I deficient. For the 15 galaxies we have measured in those groups, we obtain $\overline{def} = 0.14 \pm 0.07$, i.e. no deficiency at all. Now we can examine the location of the objects of our sample, which present the lowest H I content, i.e. those having the lowest *def* values. If we proceed this way for the 15 galaxies having $def < -0.20$, we find that 10 of them are located at random, and their negative *def* values are likely to correspond to the normal dispersion of that parameter around its zero mean. However, the other five are found in the same group of galaxies, namely group 7. In Table 5, we display the *def* values for all the 13 galaxies of this group measured in H I: nine have been measured by us, three by KH and one by Fisher & Tully (1981). One can see that all but two *def* values are negative, which points indeed towards a systematic H I deficiency in this group. The mean deficiency for these 13 galaxies is: $\overline{def} = -0.13 \pm 0.07$. That is not actually significant, but one can see that the dispersion is mainly due to the high H I content of one galaxy, namely E 430−030. One can also note that this object has the second lowest redshift and it has been included in the group mainly because its redshift is close to that of its neighbour NGC 2559. Here we face the inconvenience of Huchra–Geller grouping method, namely that at the extremity of the chain of companions, galaxies that are in fact rather questionable members can be put in a group. That is the case for E 430−030; conversely, the galaxy E 431−018 has not been included in the group, although its velocity and its position point towards an obvious membership. The reason is that its nearest companion belonging to the group, which is located at a separation smaller than the maximum one for companions, has with it a velocity difference higher than 150 km s^{-1}. So it seems to be justified to include this galaxy in group 7. Making this change, we find for the redefined group, and after removal of E 430–030, $\overline{def} = -0.20 \pm 0.05$. Now the H I deficiency is real and corresponds to a factor of 1.6.

If our result is actually significant, here we are facing the first known example of an H I deficiency in a small non-compact group of galaxies. One can think that, as for cluster galaxies, such a deficiency results from sweeping of the interstellar gas from the galaxies in their motion through an intragroup medium. If we are correct, one can then expect diffuse X-ray emission from such an intragroup medium. As far as we know, the group has not been observed in the X-ray range. However, diffuse X-ray emission has already been detected by *ROSAT* in 25 groups by Mulchaey et al. (1996). They

Table 5. H I contents of galaxies members of the group $n°7$.

Name (1)	RA (1950) (2)	Dec. (1950) (3)	V_0 (4)	log A_0 (5)	log M_H (6)	Def. (7)	Ref (8)
E430-026	$08^h12^m40^s$	$-31°11'.7$	1377	1.18	8.79	−0.27	1
CG2 2865	$08^h12^m50^s$	$-31°51'.4$	1404	0.86	8.07	−0.43	1
PGC 23156	$08^h13^m40^s$	$-28°42'.0$	1422	–	–	–	–
E430-030	$08^h14^m26^s$	$-27°58'.7$	1217	0.73	8.85	+0.59	2
E494-040	$08^h14^m52^s$	$-25°13'.0$	1237	0.80	8.05	−0.35	1
N2559	$08^h15^m01^s$	$-27°18'.1$	1287	1.45	9.25	−0.28	3
E431-001	$08^h15^m36^s$	$-29°34'.5$	1379	1.08	8.79	−0.09	1
E431-002	$08^h15^m41^s$	$-29°58'.5$	1377	1.48	9.48	−0.09	1
N2566	$08^h16^m38^s$	$-25°20'.4$	1359	1.38	9.00	−0.33	2
I2311	$08^h16^m38^s$	$-25°12'.8$	1565	–	–	–	–
E495-005	$08^h17^m07^s$	$-25°1'.9$	1398	0.80	8.34	−0.07	1
E495-006	$08^h17^m16^s$	$-24°37'.7$	1481	–	–	–	–
E495-009	$08^h19^m10^s$	$-25°36'.8$	1192	0.96	8.46	−0.22	1
E495-011	$08^h21^m11^s$	$-26°2'.1$	1429	0.84	8.72	+0.24	1
E495-012	$08^h21^m44^s$	$-25°40'.5$	1509	1.05	8.62	−0.21	1
E431-010	$08^h25^m57^s$	$-30°22'.9$	1494	0.89	8.48	−0.07	2
E431-018(*)	$08^h33^m35^s$	$-31°58'.4$	1266	1.35	8.88	−0.47	3

(*) Added group member.

Column (1) name of the galaxy: same symbols as in Table 4. (2) Right ascension (1950.0). (3) Declination (1950.0). (4) Recession velocity referred to the centroid of the Local Group (see Paper I). (5) Logarithm of the linear diameter of the galaxy in kpc, computed from the apparent diameter expressed in the ESO scale and corrected for galactic extinction as in Paper I. (6) Logarithm of the H I mass computed as in Paper I. (7) H I deficiency parameter (see the text). (8) References for H I measurements: 1, Paper I; 2, KH; 3, Fisher & Tully (1981).

have noted that those X-ray groups contain a large proportion of early-type galaxies, which could be in favour of severe gas ablation from their members, leading to a transformation of some spirals in early-type galaxies.

As a test of the possible correlation between X-ray emission and gas deficiency, we have studied five nearby groups among the X-ray ones, containing spirals observed in H I, namely groups NGC 533, 2300, 4261, 5044 and 5846. The main results are the following: galaxies of one group (NGC 4261) present a systematic H I deficiency of approximately a factor of 2, but since this group is very close to the Virgo cluster, it is possible that this H I deficiency is the general one observed in the Virgo cluster itself. In NGC 533 and 5846 groups, a strong H I deficiency (more than a factor of 3) is observed for one spiral galaxy, namely that located within the X-ray cloud. In NGC 5044 group, all the spiral galaxies are far away from the X-ray cloud (at least 500 kpc), and no H I deficiency is indeed observed. For the NGC 2300 group, only NGC 2276 lies within the X-ray cloud, and it is not H I deficient, an uncertain result, however, since NGC 2276 is tidally disturbed and its optical diameter could have been modified.

Thus a correlation between the presence of X-ray emission in a group and an H I deficiency in at least its spiral members located within the X-ray cloud seems to be quite possible. Of course, such a conclusion would need a more thorough study to be firmly settled, but it seems to favour the idea that H I deficiency in loose groups of galaxies could be in no way exceptional, at least in the X-ray emitter ones.

4 LARGE-SCALE DISTRIBUTION

4.1 An overall view

We examine the large-scale distribution of our sample galaxies in zone B (see Fig. 1).

In order to bring to light the large-scale distribution, we can use plots of galaxies for successive redshift slices, 1000 km s^{-1} wide, in the zone concerned (Figs 2a–h).

The slice $V_0 < 1000$ km s^{-1} does not merit particular comment. In turn, the slices $1000 < V_0 < 2000$ and $2000 < V_0 < 3000$ km s^{-1} (Figs 2b and c) show an obvious concentration of galaxies along an elongated structure, running from (225°, −25°) to (260°, +20°), with a second branch going from (245°, +10°) towards (245°, +35°). Such a concentration is certainly real; indeed, if the galaxy distribution was homogeneous, the maximum density of galaxies in a given sky area would be found much further on, at $V \sim 3800$ km s^{-1} for our diameter completeness limit; and incidentally, one can note that this is indeed the case in the region $l = [230°, 240°]$, $b = [+10°, +35°]$, located outside the concentration.

A careful examination of the structure shows it extends in depth mainly from 1400 to 2600 km s^{-1}; its average redshift is 2000 km s^{-1}, nearly constant along the whole structure, resulting in an average distance of 27 Mpc. The length of the structure on the sky plane is then at least 30 Mpc (the plots suggest it could extend further than the limits of zone B, a point that will be discussed below); the depth along the line of sight is 16 Mpc and the width in the sky plane is 7 Mpc. Thus its shape is of wall type, and we name this large structure the 'Puppis wall'. Note that it contains nine of the 12 groups listed in Table 2. (One should remark that this wall has been previously noted by Lahav et al. (1993) from a smaller sample of galaxies).

The Puppis wall disappears completely in the slice $3000 < V_0 < 4000$ km s^{-1} (Fig. 2d). In that slice, however, a small concentration of galaxies is notable at (260°, +30°), probably representing an extension of the Hydra cluster located at (265°, +25°), the redshift of which is $V_0 = 3400$ km s^{-1}. The next redshift slices to $V_0 = 6000$ km s^{-1} (Figs 2e and f) show some clustering of galaxies at $b > 5°$, which shifts progressively towards lower longitude values

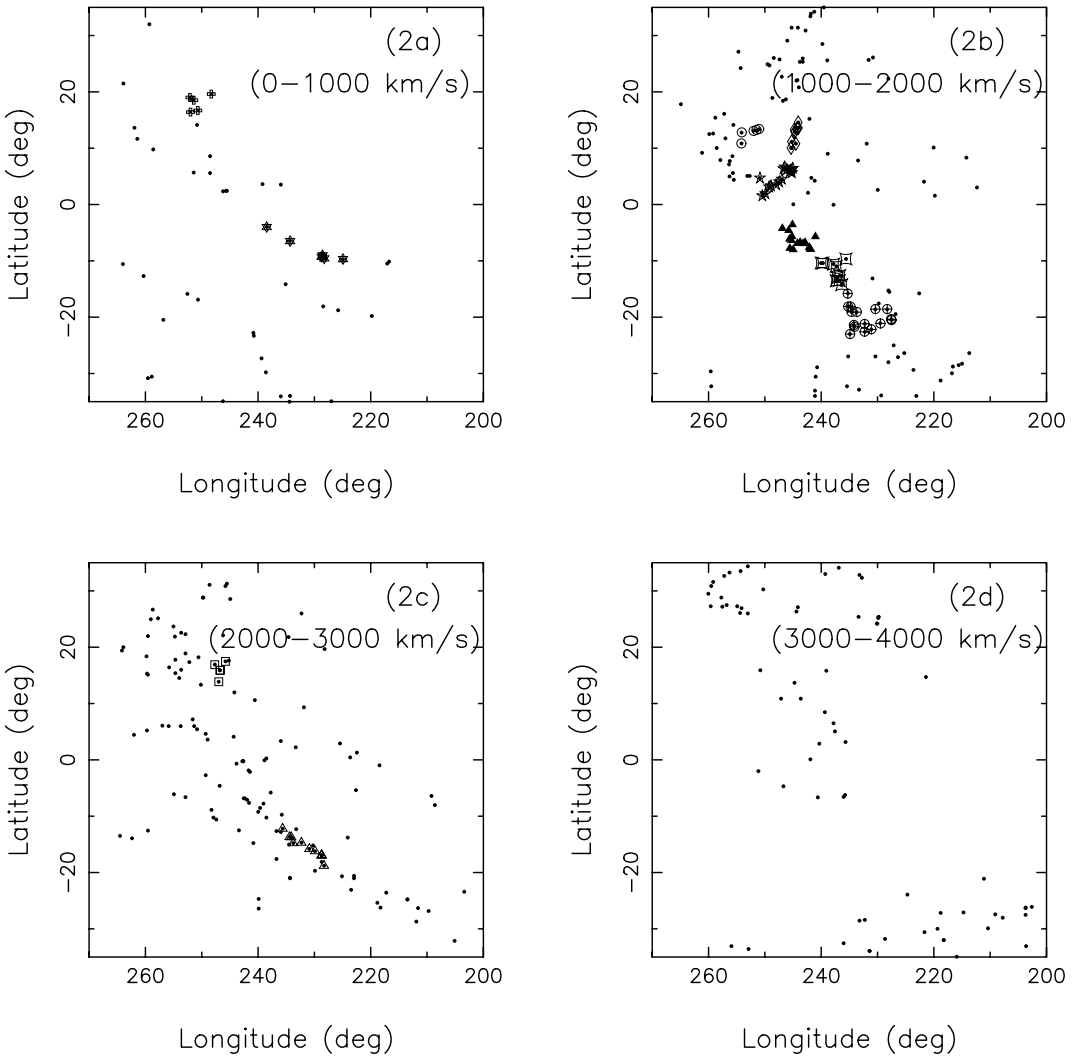

Figure 2. Cuts of our galaxy sample for successive redshift slices 1000 km s^{-1} wide, from [0, 1000 km s^{-1}] (Fig. 2a) to [7000, 8000 km s^{-1}] (Fig. 2h). Galaxies belonging to groups of at least five members are shown with symbols other than simple dots.

for increasing velocities; it could also be related to the Hydra cluster. However, the main feature appearing in the interval $3000 < V_0 < 6000$ km s^{-1} is a large void located in the zone $220^\circ < l < 260^\circ$, $-20^\circ < b < -5^\circ$; this void is real, since, in contrast, the slice $6000 < V_0 < 7000$ km s^{-1} (Fig. 2g) displays an excess of galaxies in that region. As a matter of fact, it is a part of one of the 24 voids found by El-Ad, Piran & da Costa (1997) in their analysis of the *IRAS* 1.2 Jy survey by means of an automatic algorithm especially intended to sort out voids in three-dimensional surveys. The whole corresponding void extends further than the limits of our zone, to lower l-values, namely to $l = 140^\circ$ (it is sketched nearly at the centre of their figs 2a and b, just below the trace of the galactic plane).

4.2 The Puppis wall

4.2.1 A quantitative determination

After demonstrating the Puppis wall by eye on our plots, we can now go further, and try to define it in a quantitative and objective way, in view of a more detailed study.

As any aggregate of galaxies, a wall corresponds to a region of enhanced density relative to the environment. We can find such higher density regions in the distribution of galaxies using a companionship method similar to that adopted for searching for groups; however, in the present case, contrary to what has been performed for groups, the redshift differences between galaxies will be interpreted as pure distance differences resulting from the Hubble law; indeed the internal motions within the wall due to gravitation are not significant as shown below. Note that such a treatment is not strictly valid for galaxies belonging to the same group, but will nevertheless be correct with the value adopted here for the maximum distance between companions.

Thus two galaxies i and j will be considered as companions (i.e. belonging to the same structure) if their distance d_{ij} is such that $d_{ij} \leqslant D_L$ where D_L is a limiting distance, which depends on the mean distance of the galaxies to us. d_{ij} is defined from the data by

$$d_{ij} = \left[d_{ijp}^2 + H_0^{-2}(V_i - V_j)^2\right]^{1/2},$$

where d_{ijp} is the distance between i and j projected on the sky plane, V_i and V_j being the recession velocities of i and j, respectively.

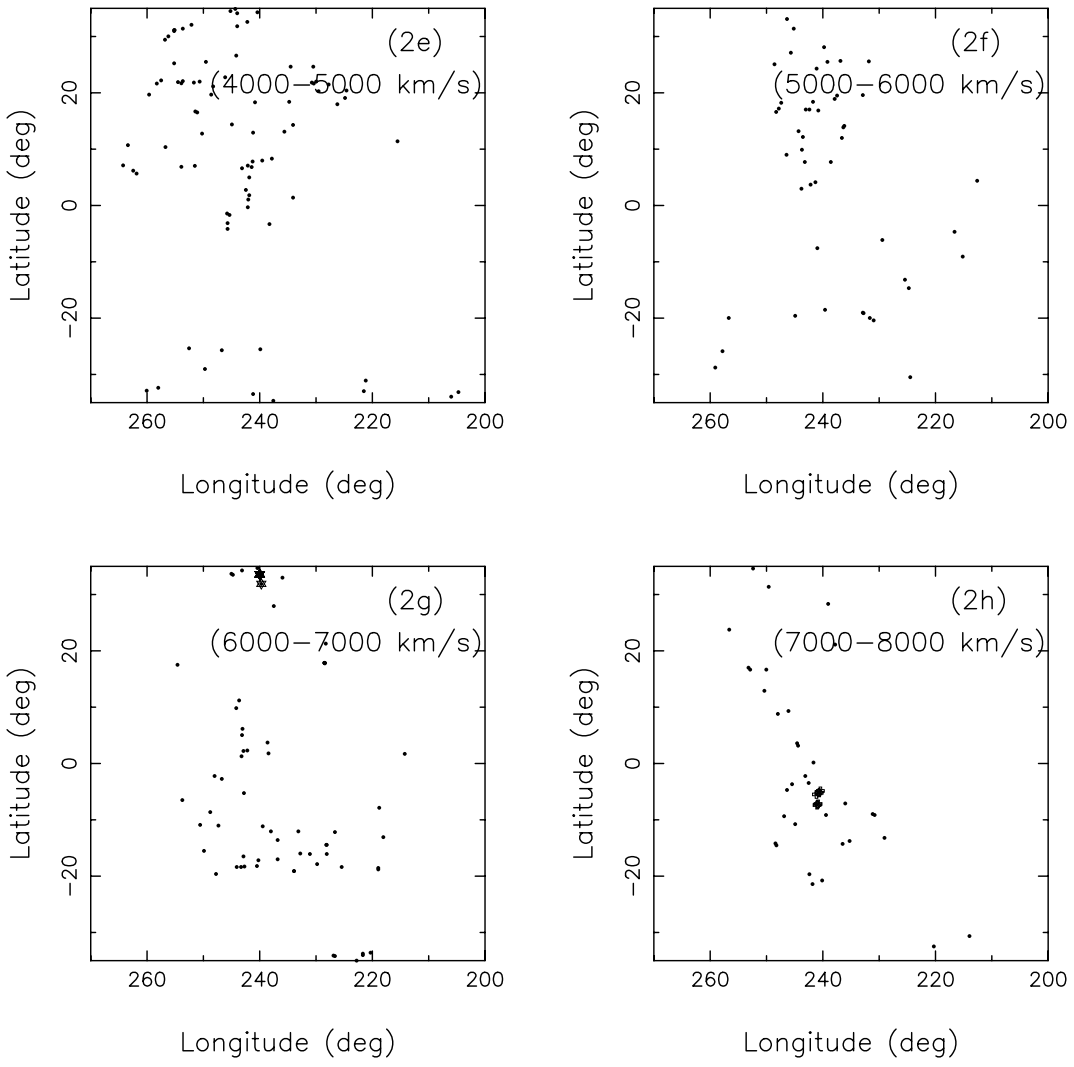

Figure 2 – *Continued*

As in the search for groups, D_L has to be scaled with distance, in order to insure that a given structure is not modified when put at a different distance from us. More precisely, let us consider a structure found by the method and located at the distance Δ_1; let us imagine moving that structure and its environment at the distance $\Delta_2 > \Delta_1$. Since the galaxy sample is complete in apparent diameters, there will be fewer galaxies of the sample present in the structure at Δ_2 than at Δ_1. However, we require that those remaining galaxies are still recognized by the method as an independent structure (and of course we have the same requirement if the structure is moved at a distance $\Delta_3 < \Delta_1$). As shown in GCF, a sufficient condition in order to satisfy such a requirement is that the number n of companions of any galaxy does not depend on its distance Δ to us as long as that galaxy is included in the sample (it disappears from the sample for too large Δ). For a sample complete to an apparent diameter a_0, n varies with Δ (or with $V = \Delta/H_0$) as $n \propto \Phi(\geqslant a_0 V)\, D_l^3(V)$ since n is the number of galaxies of the sample included in the sphere of radius $D_l(V)$ centred on the galaxy, $\Phi(\geqslant a_0 V)$ being the cumulative linear diameter function. Thus the scaling of D_l with V is given by $D_l(V) \propto [\Phi(\geqslant a_0 V)]^{-1/3}$.

Here $a_0 = 1.9$ arcmin, and for Φ we use Lahav et al.'s (1988) diameter function, as in the search for groups. In order to sort out structures, we just have to fix D_l for a given value of V, for instance $V_0 = 1000$ km s^{-1}.

We have looked for the minimal value of $D_l(1000)$ leading to the Puppis wall as has been demonstrated by visual examination of the maps. This corresponds to $D_l(1000) = 2.6$ Mpc. For this value, we find two main large-scale structures.

(i) S_1 : $\langle V \rangle = 1790$ km s^{-1}, 197 galaxies, V in the range (1039, 2610 km s^{-1}).

(ii) S_2 : $\langle V \rangle = 677$ km s^{-1}, 40 galaxies, V in the range (434, 1047 km s^{-1}).

For $D_l = 2.8$ Mpc, (S_1) and (S_2) are merging in a structure containing 244 galaxies, i.e. with only seven galaxies more than the sum of the populations of (S_1) and (S_2) found for $D_l = 2.6$ Mpc, and which presents the same limits in redshifts. At $D_l = 2.4$ Mpc, the galaxies of (S_1) at $b \geqslant 25°$ are lost. So the structure (S_1) (the Puppis wall) appears quite stable as far as the limits in velocities are concerned. It is related to an aggregate (S_2) of nearby galaxies, but the connection between the two structures seems to be spatially quite narrow.

Thus the Puppis wall is well defined quantitatively, in agreement with the visual examination of the maps.

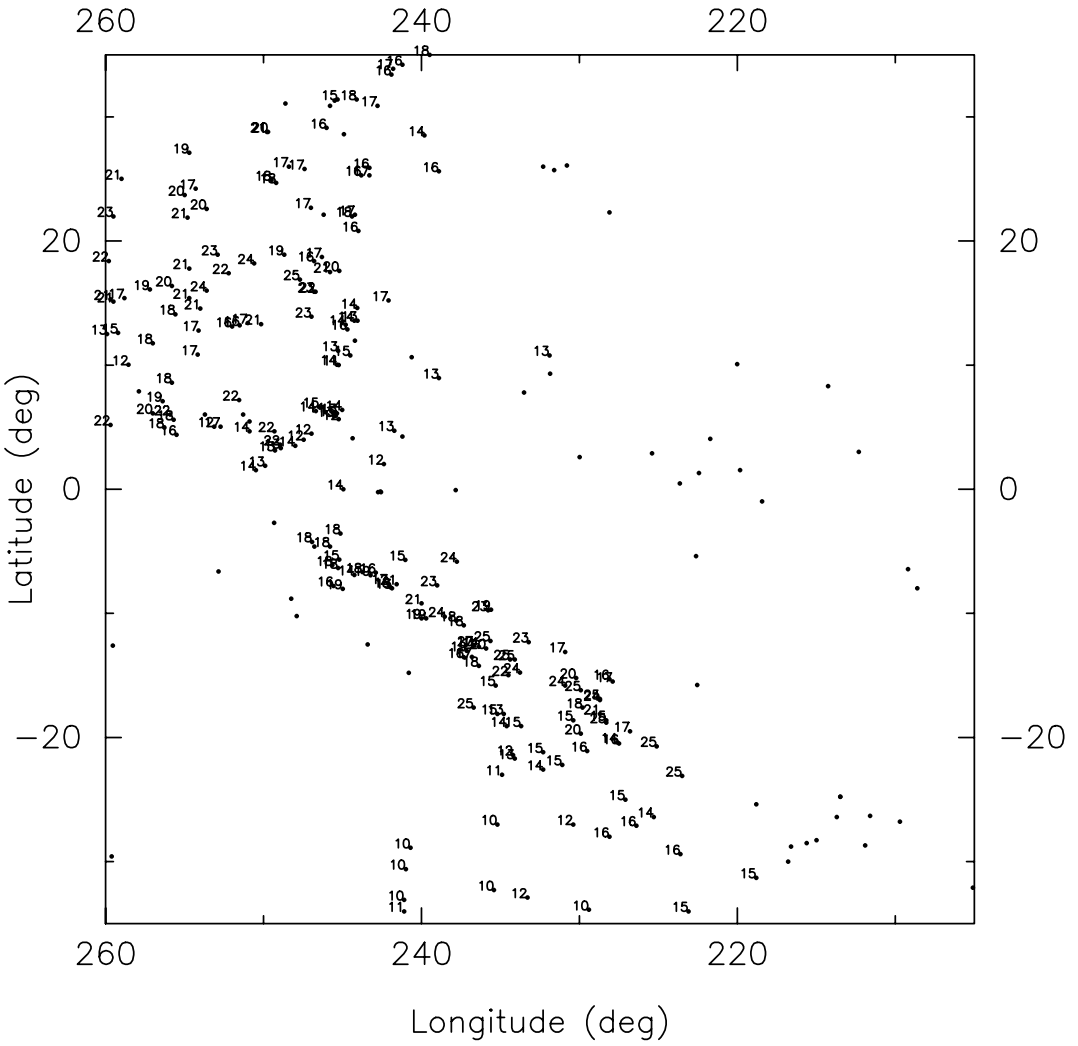

Figure 3. The Puppis wall found using the neighbourhood method with a maximal distance between neighbours $D_L = 2.6$ Mpc at $V_0 = 1000$ km s^{-1}. Galaxies included in the wall have their recession velocities noted just at the left of their position, in units of 100 km s^{-1}. Galaxies without noted velocities do not pertain to the wall, although they have velocities in the same range as those in the wall.

A plot of the galaxies of this wall including their velocities is presented in Fig. 3, which confirms the description of the structure given above.

At that stage, we can briefly return to the use of the companionship method in the case of galaxies belonging to groups. In such a case, the redshifts are not exactly proportional to the distance, but present a component due to internal motions within the group. The best way to proceed with those group galaxies in the companionship method would be to replace their recession velocity by that of the group they belong to. However, that refinement is not needed in the present case, because it occurs that if one group galaxy belongs to the Puppis wall, then all the galaxies of this group are included in it by the companionship method. Indeed, let us assume first that the group is at $V = 1000$ km s^{-1}; if i and j are companions in the group definition, that means: $d_{ijp} < 0.84$ Mpc, and $|V_i - V_j| < 150$ km s^{-1} (see Section 3.1). Then the distance d_{ij} computed in the present companionship method is $d_{ij} < 2.2$ Mpc, which is lower than the maximum distance between companions $D_l = 2.6$ Mpc adopted for the Puppis structure; so if i is in the Puppis filament, j is also in it. If the group velocity increases, one can easily see that the maximum value of d_{ij} between companions in the group sense increases less quickly than $D_l(V)$, so i and j are a fortiori companions in Puppis; since 1000 km s^{-1} is the lower velocity limit in the Puppis filament, that resolves our point.

As a matter of fact, one finds that all the groups, the coordinates and velocities of which are in the range covered by the Puppis wall, are actually included in that structure by our companionship method, in particular the nine groups with at least five members and having $1000 \leqslant V \leqslant 2600$ km s^{-1}.

More precisely, the population of 197 galaxies of the Puppis wall in the zone studied is comprised of 143 galaxies (i.e. 73 per cent) belonging to 26 of our groups of three members at least or to pairs, and 54 galaxies not associated to any group or pair.

4.2.2 Real extension of the Puppis wall

As shown in Fig. 3, the Puppis wall could extend beyond the limits of zone B, namely beyond the points (245°, +35°), (260°, +15°) and (220°, −35°).

As a matter of fact, no significant extension of the Puppis wall appears at $b > +35°$, $l \sim 245°$, from redshift surveys by Chamaraux & Siemieniec (1991) and by Davis et al. (1982).

Concerning a possible extension beyond $l > 260^\circ, b \sim +15^\circ$, one can note the presence of the Antlia cluster at (273°, +19°) with a recession velocity $V_0 = 2640$ km s^{-1}. The recession velocity of the Puppis wall at (260°, +15°) is $V_0 \sim 2000$ km s^{-1}. Examination of the figures given by da Costa et al. (1994) and by Kraan-Korteweg, Fairall & Balkowski (1995) indeed shows a continuity in recession velocities between the Puppis wall and the Antlia cluster, indicating that the two structures are actually connected. According to Henning et al.'s (1999) study, the wall could even extend well beyond the Antlia cluster; indeed they trace it at increasing l and decreasing b up to $l \sim 380^\circ$, through the Centaurus cluster and a second crossing of the galactic plane. However, at $l > 280^\circ$, recession velocities of galaxies in the structure are higher, being mainly included in the interval [2500, 3500 km s^{-1}].

One can now examine the possible extension of the wall beyond $(l, b) = (230^\circ, -35^\circ)$ using Fairall's (1995) data. As a matter of fact, the data show a real extension up to the two clusters Eridanus ($V_0 = 1600$ km s^{-1}) and Fornax ($V_0 = 1380$ km s^{-1}) each being mutually connected. Thus it seems that the Antlia cluster on one hand, and Fornax and Eridanus clusters on the other hand, are connected through the Puppis wall. In such a case, the Puppis wall would be 90° long at least in the plane of the sky; redshifts increase gradually in it from 1500 km s^{-1} at $b = -40^\circ$ to 2600 km s^{-1} at $b = +20^\circ$; so its average distance is approximately 27 Mpc and then its length is 40 Mpc; the depth along the line of sight is 1300 km s^{-1} (17 Mpc) and its width on the sky plane is ∼15°, i.e. 7 Mpc, as found above. Thus it is quite elongated and its wall geometry is confirmed. If one adds the part given by Henning et al. (1999) at $l > 280^\circ$, we obtain a structure with an extension of 210°, i.e. as long as 100 Mpc (compared with 70 Mpc for the Pisces–Perseus supercluster length).

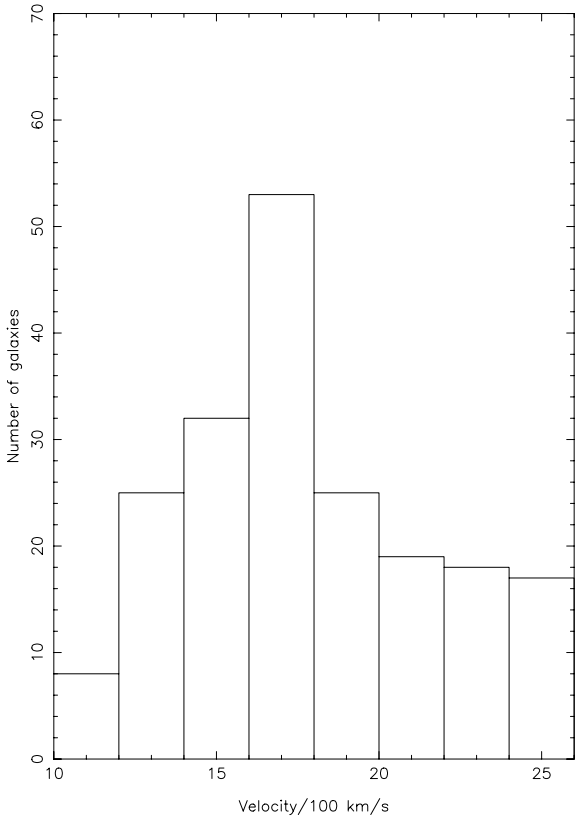

Figure 4. Histogram of the recession velocities of the 197 galaxies included in the Puppis wall.

4.2.3 Density of galaxies within the Puppis wall

First, in Fig. 4 we give the histogram of the recession velocities of galaxies within the Puppis wall. This histogram has been drawn assigning the mean velocity of the group to each galaxy included in a group; this is more convenient if one wishes the histogram to reflect the distance distribution within the wall. One can go even further, and try to derive the distribution of the galaxy densities within the wall from the velocity histogram; for that purpose, we have to know approximately the geometrical shape of the structure; judging from cuts at different redshifts perpendicular to the line of sight, it seems that the surface it covers in those cuts is roughly constant. If this is so, slices in redshifts having the same depths cut equal volumes in the structure, and since our sample is complete in apparent diameters, we derive the total density in galaxies $\rho(V)$ from the velocity histogram $N(V)$ by $\rho(V) \propto N(V)\ [\Phi(\geqslant a_0 V)]^{-1}$ since $N(V)$ is the number of galaxies in the redshift slice $(V, V + \Delta V)$ having a linear diameter larger than $a_0 V$ (also see equation 1, Section 2.2).

The actual densities will be determined just below. Here, we give in Fig. 5 the distribution of the galaxy density in the wall, within a constant multiplicative factor. Interestingly, except for a narrow peak at 1600–1700 km s^{-1}, this density is nearly constant from 1200 to 2500 km s^{-1}, and equal to half the peak value.

This leads to the following questions: what is the actual density of galaxies in the Puppis wall and, especially, what is its overdensity compared with the general field? And how does it compare to other similar structures, the Pisces–Perseus filament for instance? Here we try to answer those questions.

As already stated, redshifts are taken as distance measurements within the structure, an assertion that will be justified below. Note that this is not entirely correct for the group galaxies but internal velocities in the groups are small compared with the velocity range covered by the wall. Also note that we compute the mean galaxy density of the wall, but the density is quite variable within the structure, being in particular much higher in the groups; so we also separately determine the density in the groups and in the intergroup region as well.

First, we have to define the sample of galaxies we use for the computation of the density. Indeed, we cannot use the whole sample of wall galaxies, since it is complete in apparent diameters only, and the apparent diameter is not a physical characteristic of the galaxies. Instead, we need to use a subsample that is complete in linear diameters. The largest complete subsample of this kind is defined by the limiting lower linear diameter A_0, which is seen under an angle of $a_0 = 1.9$ arcmin – the completeness apparent diameter – at the maximum velocity of 2600 km s^{-1} reached within the wall. Therefore, the subsample used is comprised of all the wall galaxies having a diameter $A \geqslant A_0 = 4940$ arcmin x km s^{-1} (approximately 19 kpc here).

We have to determine the proportion of wall galaxies pertaining to that subsample. Obviously, that proportion varies with distance. In each velocity interval $(V, V + \mathrm{d}V)$, the number of galaxies $\mathrm{d}n(V)$ belonging to the subsample is given by

$$\mathrm{d}n(V) = \left[\mathrm{d}N(V)\frac{\Phi(\geqslant A_0)}{\Phi(\geqslant a_0 V)}\right],$$

where $\mathrm{d}N(V)$ is the number of galaxies of the wall having recession velocities in $(V, V + \mathrm{d}V)$.

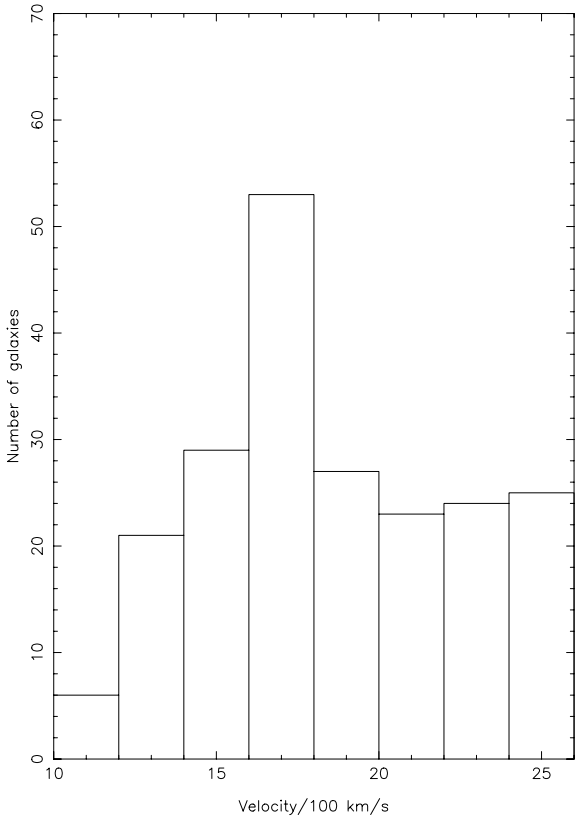

Figure 5. Galaxy density (within a constant multiplicative factor) in the Puppis wall as a function of the recession velocity.

This formula allows computation of the total number n of galaxies in the wall subsample from the velocity histogram of Fig. 4, which gives $dN(V)$ for successive adjacent velocity intervals 200 km s^{-1} wide. We find $n = 120$; so 61 per cent of the 197 galaxies within the wall belong to the subsample defined above.

As seen in Fig. 3, the wall is comprised of two parts: a dense oblique narrow band, extending from $b = -20^\circ$ to 0°, which occupies approximately 30×7 deg^2 on the sky, and a second part, at $l \geqslant 240^\circ$ and $b \geqslant 0^\circ$, approximately 30×15 deg^2 in extent. Thus the total area covered by the wall in the sky plane is approximately 660 deg^2. The average recession velocity and the velocity range are 1800 and 1300 km s^{-1}, respectively; so the volume occupied by the wall is approximately 2000 Mpc^3. Hence its mean density in galaxies having a linear diameter larger than A_0 is: $\rho(\geqslant A_0) = 120/2000 = 0.060$ Mpc^{-3}.

The general average density of ESO galaxies with diameters larger than A_0 can be computed from Lahav et al.'s (1988) cumulative diameter function: $\langle\rho(\geqslant A_0)\rangle = 0.718\Phi_*$ with $\Phi_* = 0.0048$ Mpc^{-3} for $H_0 = 75$ km s^{-1} Mpc^{-1}. Hence $\langle\rho(\geqslant A_0)\rangle = 0.0034$ Mpc^{-3}.

Thus the overdensity in the wall amounts to a factor of 18.

4.2.4 Density variations within the wall

First, we can note that the companionship method provides the value of the lowest local density found within the wall. Indeed, there is always one companion at least in the sphere of radius $D_l(V)$ centred on any wall galaxy having a recession velocity V. At $V = 2600$ km s^{-1}, one only selects from this sphere those galaxies having $A \geqslant A_0$; one has $D_l(2600) = 3.4$ Mpc, resulting in the lowest possible density $\langle\rho_l(\geqslant A_0)\rangle = 2/v_l = 0.013$ Mpc^{-3}, around each wall galaxy, where $v_l = (4/3)\pi(3.4)^3$. Note that the companionship spheres cut each other 2 by 2, and then form a continuous volume; in fact the set of these spheres is the best representation of the volume occupied by the wall; so each point of the wall lies within such a companionship sphere, and ρ_l then represents actually the lowest limit of the density found anywhere in the wall, a value that is still 4 times higher than the average density of ESO galaxies.

The regions of the wall occupied by the groups are among those having the highest densities; this is so since the maximum distance between companions in a given group is lower than that between companions in the wall, as shown above. As already noted, there are 26 groups and pairs in the wall; we can compute the volume of each group or pair assuming it is spherical, centred on its centre of mass G and with a radius $R_{\max} = \max(R_{iG})$, which is the maximum distance of any of its members to G (see GCF for more details). The total volume covered by the groups and the pairs is then equal to 420 Mpc^3, i.e. one-fifth of the total volume of the wall, and they contain 70 per cent of the wall members. Assuming the same proportion of galaxies having $A \geqslant A_0$ in the groups as in the whole wall leads to a mean group density $\overline{\rho_G} = 86/420 = 0.20$ Mpc^{-3}; the mean intergroup density is then $\overline{\rho_i} = 34/1580 = 0.021$ Mpc^{-3}.

Therefore, the group density is approximately 60 times the average general galaxy density and 10 times the intergroup density. Note that the intergroup density is approximately twice the lowest density found in the wall.

At this stage it is worthwhile comparing our density values in the Puppis wall to those found in the well-known Pisces–Perseus (PP) filament. Wegner, Haynes & Giovanelli (1993) have carried out a detailed study of the main PP supercluster ridge, from the redshift measurements. We have determined the galaxy density in that part of the ridge selected by Eisenstein, Loeb & Turner (1997), which is one of the densest in the PP filament; its corners are (0^h30^m, 27°), (2^h15^m, $36^\circ.5$), (2^h15^m, $40^\circ.5$) and (0^h30^m, 31°); it contains 307 galaxies of Wegner et al.'s (1993) sample having corrected recession velocities in the range of the supercluster ones (namely $4200 < V_0 < 6000$ km s^{-1}); the average recession velocity of the filament at this place is $\overline{V} = 5100$ km s^{-1} (as in Puppis, we use recession velocities referred to the centre of the Local Group).

As shown in Wegner et al. (1993), the defined sample is complete in apparent diameters to the UGC limit $a_U = 1.0$ arcmin, resulting in a completeness in the ESO scale to $a_1 = 1.1$ arcmin from the relation between UGC and ESO diameters found by Lahav et al. (1988).

Thus we can proceed as for the Puppis wall in order to compute density in galaxies, taking advantage of the diameter completeness of the sample. We find $\rho_{PP}(\geqslant A_0) = 0.13$ Mpc^{-3}, that is twice the galaxy density in the Puppis wall.

Note that the PP density computed here corresponds to one of the regions of the highest densities in the supercluster, characterized notably by the presence of two rich clusters. In fact, although Puppis is less prominent than PP, it also appears as a well characterized structure.

Also note that in the computation, we have taken the redshifts dispersion found in PP as solely resulting from Hubble expansion; so we have neglected the internal motion within PP, in the same way as we have proceeded in Puppis. However, according to Eisenstein et al. (1997), in contrast, internal motions are mainly responsible for the redshift dispersion in PP. As shown below, that is not the case in Puppis, and in PP the evidence is inconclusive. However, if Eisenstein et al. (1997) are right, the depth of the PP filament

would be much smaller, being of the order of its width, that is approximately 4 Mpc. In this case, $\rho_{PP}(\geqslant A_0) \sim 0.78$ Mpc^{-3}, i.e. 13 times the Puppis density.

4.2.5 Origin of the redshift dispersion within the Puppis wall

It is important to determine whether the redshift dispersion within the Puppis wall results from internal gravitational motions or from the Hubble expansion. At first because the result conditions the actual value of the galaxy density; then, still more important, if the internal motions are predominant within a structure such as Puppis where the main axis is perpendicular to the line of sight, one can compute its total mass from its redshift dispersion, using an ingenious method devised by Eisenstein et al. (1997) and applied by them to the Pisces–Perseus filament.

The check of the origin of the redshift dispersion in the Puppis structure is possible in principle. Indeed, the redshift range [1300–2600 km s^{-1}] corresponds to a ratio of 2 in the distances if it results from Hubble expansion, a large enough value to be easily brought to light.

We perform the check from the Tully–Fisher (TF) linear relation between logarithms of the maximum rotational velocity V_m and of the linear diameter A of a spiral galaxy (Tully & Fisher 1977). Thus we limit to those Puppis objects for which V_m has been determined, that is those measured in the 21-cm H I line.

We proceed comparing the distances of two Puppis subsamples of galaxies where the redshifts are different and cover respective narrow ranges, namely [1300–1500 km s^{-1}] and [1800–2200 km s^{-1}]. For each of those subsamples, we plot $\log(a_c)$ versus $\log(2V_m)$; since galaxies within a given subsample are located at the same distance, the two plots are expected to be straight lines parallel to the TF relation. If the velocity dispersion in Puppis results from internal motions, then the two subsamples are at the same distance from us and they follow a unique [$\log(2V_m)$, $\log(a_c)$] relation. However, if the velocity dispersion results from the Hubble expansion, the two subsamples are located at different distances, and they follow distinct [$\log(2V_m)$, $\log(a_c)$] relations that are shifted from each other by the logarithm of the ratio of their average respective recession velocities.

The H I and diameters data used come from Paper I, resulting in 12 and 18 objects in the subsamples at low and high velocities, respectively. V_m has been determined from the H I profile width exactly as performed by KH.

Fig. 6 displays the [$\log(2\,V_m)$, $\log(a_c)$] relations obtained for the two subsamples of Puppis galaxies. The two relations are clearly distinct, leading to a distance ratio between the two groups:

$$\left\langle \log \frac{\Delta_2}{\Delta_1} \right\rangle = 0.32 \pm 0.13$$

i.e. approximately a factor of 2; the velocity ratio is

$$\left\langle \log \frac{V_2}{V_1} \right\rangle = 0.19 \pm 0.01$$

That is compatible with the Hubble law through the uncertainties. In turn, the result is not compatible with the same distances for the two samples (2.5 times the dispersion).

Thus the Hubble expansion is the cause of the redshift dispersion within the Puppis structure (except of course within the groups), and no internal motion is apparent out of the groups. This means that, except in the groups, the Puppis structure is not yet collapsing and that one cannot compute its mass using Eisenstein et al.'s (1997) method. On the other hand, such a result confirms the wall shape of the structure.

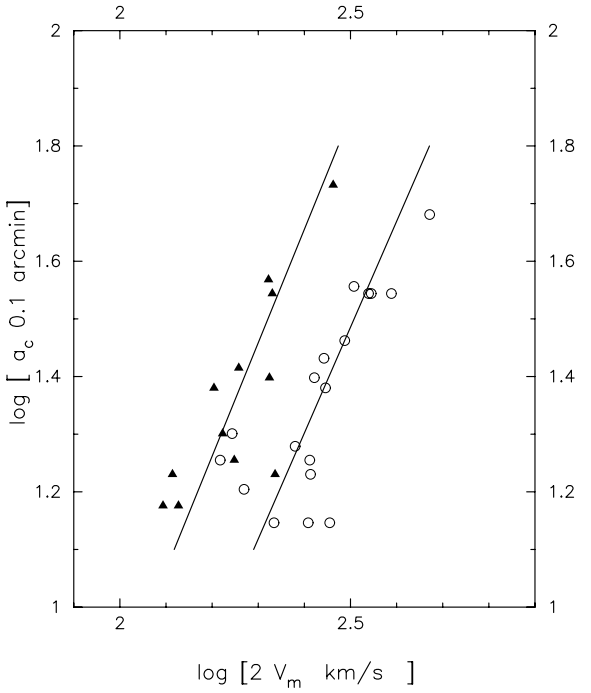

Figure 6. Plot of the apparent diameter a_c versus $2V_m$, where V_m is the maximum rotational velocity of the galaxy; the plot is shown for two sets of galaxies in the Puppis wall, at recession velocities [1300 < V_0 < 1500 km s^{-1}] (triangles) and [1800 < V_0 < 2200 km s^{-1}] (circles), respectively. Least square regression lines are drawn for each set of points.

We end this section with the following two remarks.

(i) The fact that the Puppis structure is not yet collapsing is likely to be due to a too low density. As a matter of fact, the density at turnaround of a collapsing filament is approximately six times the background density in an $\Omega = 0.4$ universe (Eisenstein et al. 1997) and the average density of the Puppis structure in the intergroup region has just this value, showing why collapse has not yet been initiated here.

(ii) We have tried to perform the same test for Hubble expansion in the Pisces–Perseus supercluster, but it has been inconclusive; indeed, since the supercluster is much more remote than Puppis, one has to look for distance variations of approximately 30 per cent, which is not possible to bring to light given the accuracy of the data. As we have seen above, if the redshift dispersion comes from Hubble expansion, then the average density in the densest part of the PP ridge is twice that in Puppis, thus allowing collapse. However, it is not possible to state that PP is collapsing because there are rich clusters and groups in the region considered, and one needs to determine the intercluster density to be able to reach a firm conclusion. Finally, it is perhaps significant to note that Wegner et al. (1993) have computed a general overdensity of a factor of 6 in the whole PP ridge compared with the background density, assuming that for this determination there is Hubble expansion within the supercluster; this would imply that collapse has indeed not yet begun in the PP ridge as a whole.

CONCLUDING REMARKS

The spatial distribution of galaxies has been studied in the part of the zone of avoidance: $220^\circ < l < 260^\circ$, $|b| < 20^\circ$, $\delta \leqslant 0^\circ$,

$V_0 < 8000$ km s^{-1}, from a sample of 369 objects with known redshifts, of which 97 have been measured in the H I line with the Nançay radio telescope. Distances of galaxies have been simply derived through the Hubble law. We have shown that our sample is equivalent to a complete one, in apparent diameter to 1.9 arcmin, in the major part of the zone, a property that allows us to correct the density in galaxies from the loss of objects for increasing distances; such a correction becomes important at large distances, so that the distribution of galaxies can be confidently determined up to 3000 km s^{-1} only.

In the first step, groups were looked for in the zone investigated, using HG's improved companionship method. 11 groups with at least five members were found at $V_0 < 2600$ km s^{-1}, of which four had not been noted previously. The galaxies of one of those groups seem to be systematically H I deficient by a factor of 1.6 on average, indicating the possible presence of intragroup gas; it would be interesting to check the presence of this gas by looking for its X-ray emission.

In a second step, large-scale structures were looked for using a three-dimensional companionship method. As a result, an important structure, the Puppis wall, has been demonstrated; it goes across the whole zone studied, through the galactic equator. Its major axis is parallel to the sky plane. Its length is 30 Mpc and it extends from 1400 to 2600 km s^{-1} along the line of sight. It seems to connect the Antlia and the Fornax clusters, through the obscuration zone. The full length could then be up to 100 Mpc. The density in galaxies within this structure is 18 times as large as the average density of ESO galaxies, and half that found in the densest region of the Pisces–Perseus supercluster.

We have not found evidence for any internal motions along the line of sight, which suggests that the Puppis wall has not yet collapsed along that direction.

It would be interesting to provide a better specification of the structure of the Puppis wall and of its surroundings, in particular by increasing the sample of galaxies in the zone $-7^\circ < b < +4^\circ$, $220^\circ < l < 235^\circ$ and $250^\circ < l < 260^\circ$, which could provide useful data to explain the peculiar velocity of the Local Group perpendicular to the Supergalactic Plane.

REFERENCES

Chamaraux P., Siemieniec G., 1991, in Mamon G.A., Gerbal D., eds, 2nd DAEC Meeting, The Distribution of Matter in the Universe. Observatoire de Paris, Paris, p. 179

Chamaraux P., Masnou J.L., Kazés I., Saitō M., Takata T., Yamada T., 1999 MNRAS, 307, 236 (Paper I)

da Costa L.N. et al., 1994, ApJ, 424, L1

Davis M., Huchra J., Latham D.W., Tonry J., 1982, ApJ, 253, 423

de Vaucouleurs G., de Vaucoulers A., Corwin H.G., 1976, Second Reference Catalog of Bright Galaxies. Univ. Texas Press, Austin

Eisenstein D.J., Loeb A., Turner E.L., 1997, ApJ, 475, 421

El-Ad H., Piran T., da Costa L.N., 1997, MNRAS, 287, 790

Fairall A.P., 1995, Southern Redshift Catalogue. Dep. Astron., Univ. Cape Town

Fisher J.R., Tully R.B., 1981, ApJS, 47, 139

Fisher K.B., Huchra J.P., Strauss M.A., Davis M., Yahil A., Schlegel D., 1995, ApJS, 100, 69

Fouqué P., Gourgoulhon E., Chamaraux P., Paturel G., 1992, A&AS, 93, 211

Gourgoulhon E., Chamaraux P., Fouqué P., 1992, A&A, 255, 69 (GCF)

Haynes M., Giovanelli R., 1984, AJ, 89, 758

Henning P.A., Staveley-Smith L., Kraan-Korteweg R.C., Sadler E.M., 1999, PASA, 16, 35

Huchra J.P., Geller M.J., 1982, ApJ, 257, 423 (HG)

Hudson M.J., Lynden-Bell D., 1991, MNRAS, 252, 219

Jensen J.B., Tonry J.L., Thompson R.I., Ajhar E.A., Lauer T.R., Rieke M.J., Postman M., Liu M.C., 2001, ApJ, 550, 503

Kolatt T., Dekel A., Lahav O., 1995, MNRAS, 275, 797

Kraan-Korteweg R.C., Huchtmeier W.K., 1992, A&A, 266, 150 (KH)

Kraan-Korteweg R.C., Lahav O., 2000, ARA&A, 10, 211

Kraan-Korteweg R.C., Fairall A.P., Balkowski C., 1995, A&A, 297, 617

Lahav O., Rowan-Robinson M., Lynden-Bell D., 1988, MNRAS, 234, 677

Lahav O., Yamada T., Scharf C., Kraan-Korteweg R.C., 1993, MNRAS, 262, 711

Materne J., 1978, A&A, 63, 401

Mulchaey J.S., Davis D.S., Mushotzky R.F., Burstein D., 1996, ApJ, 456, 80

Pellegrini P.S., da Costa L.N., Huchra J.P., Latham D.W., Willmer C.N.A., 1990, AJ, 99, 751

Ponman T.J., Bourner P.D.J., Ebeling H., Böhringer H., 1996, MNRAS, 283, 690

Saitō M., Ohtani H., Asonuma A., Kashikawa N., Maki T., Nishida S., Watanabe T., 1990, PASJ, 42, 603

Saitō M., Ohtani H., Baba A., Hotta H., Kameno S., Kurosu S., Nakada K., Takata T., 1991, PASJ, 43, 449

Tully R.B., 1987, ApJ, 321, 280

Tully R.B., Fisher J.R., 1977, A&A, 54, 661

Visvanathan N., Yamada T., 1996, ApJS, 107, 521

Wegner G., Haynes M.P., Giovanelli R., 1993, AJ, 105, 1251

Williams B.A., Rood H.J., 1987, ApJS, 63, 265

Yamada T., Takata T., Djamaluddin T., Tomita A., Aoki K., Takada A., Saitō M., 1993, ApJS, 89, 57

Yamada T., Tomita A., Saitō M., Chamaraux P., Kazés I., 1994, MNRAS, 270, 93

This paper has been typeset from a TEX/LATEX file prepared by the author.